JOURNAL OF VIROLOGY, Aug. 2007, p. 8293–8302 Vol. 81, No. 15
0022-538X/07/$08.00+0 doi:10.1128/JVI.00266-07

The F Gene of Rodent Brain-Adapted Mumps Virus Is a Major Determinant of Neurovirulence▽

Ken Lemon,[1] Bertus K. Rima,[1] Stephen McQuaid,[2] Ingrid V. Allen,[1] and W. Paul Duprex[1]*

School of Biomedical Sciences, The Queen's University of Belfast, 97 Lisburn Road, Belfast, United Kingdom BT9 7BL,[1] and Neuropathology Laboratory, Royal Group of Hospitals Trust, Belfast, United Kingdom BT12 6BL[2]

Received 7 February 2007/Accepted 26 March 2007

Prior to the introduction of live-attenuated vaccines, mumps virus (MuV) was the leading cause of virus-induced meningitis. Although vaccination has been effective at controlling the disease, the use of insufficiently attenuated strains has been associated with high rates of aseptic meningitis in vaccinees. The molecular basis of MuV attenuation is poorly understood, and no reliable molecular markers of virulence have been identified. In this study, reverse genetics has been used to identify molecular determinants of MuV neuropathogenesis. Recombinant viruses, containing the envelope-associated genes from the Kilham (MuV^{KH}) rodent brain-adapted strain of MuV, were generated in the Jeryl Lynn 5 (MuV^{JL5}) vaccine strain background. The syncytium phenotypes of the recombinant viruses on Vero cells differed depending on the source of the fusion (F) and hemagglutinin-neuraminidase (HN) glycoproteins, with heterologous combinations showing either an increase or a decrease in the level of cell fusion compared to that of the homologous parental combinations. This was confirmed by transiently cotransfecting eukaryotic F and HN glycoprotein expression constructs. A Lewis rat model that discriminates between neurovirulent and nonneurovirulent MuV strains based on the extent of hydrocephalus induced in the rat brain after intracerebral inoculation was used to assess the phenotype of the recombinant viruses. Expression of the matrix (M), small hydrophobic (SH), or HN gene in isolation did not confer a neurovirulent phenotype. Expression of the F gene of the neurovirulent strain alone was sufficient to induce significant levels of hydrocephalus. Coexpression of the homologous HN gene led to a marginal increase in the level of hydrocephalus.

Mumps virus (MuV) is a member of the *Rubulavirus* genus of the family *Paramyxoviridae*. The virus contains a negative-sense RNA genome of 15,384 nucleotides that consists of seven transcription units. The gene order is as follows: nucleoprotein (N), phosphoprotein (P), and matrix (M), fusion (F), small hydrophobic (SH), hemagglutinin-neuraminidase (HN), and large (L) proteins. Each gene encodes a single protein with the exception of the second, which encodes three proteins (V, P, and I) via RNA editing (31). Transcription units are flanked by 3′ and 5′ untranslated regions (UTRs) containing consensus gene start (GS) and gene end (GE) signals and are separated by intergenic sequences of 1 to 7 nucleotides (17). MuV virions consist of an inner helical ribonucleoprotein (RNP) core surrounded by an envelope that is derived from the host plasma membrane. The RNP is composed of the viral RNA encapsidated with N protein and associated with L and P proteins, which together form the RNA-dependent RNA polymerase. The F protein is a type I glycoprotein, synthesized as an inactive precursor (F_0) that is subsequently cleaved into two polypeptides (F_1 and F_2) which remain linked by a single disulfide bond. HN is a type II integral membrane protein. The F and HN glycoproteins are inserted into the viral envelope and are responsible for receptor recognition and entry. The M protein is membrane associated and plays important roles in viral assembly and budding. MuV also encodes a 57-amino-acid SH integral membrane protein of unknown function. This has recently been shown to have antiapoptotic activity (48), but like other small viral proteins, it may be multifunctional.

Recent mumps epidemics in both the United States (20) and the United Kingdom (11) demonstrate that the disease remains clinically relevant in the developed world. MuV can be successfully controlled by the use of live-attenuated virus vaccines. The Jeryl Lynn strain of MuV, originally isolated from the daughter of a prominent virologist (9), was adapted to growth in embryonated chicken eggs and became attenuated in monkeys (18). This strain was subsequently developed as a vaccine and was licensed in the United States in 1967. The vaccine has been shown to be a mixture of two closely related viruses, Jeryl Lynn 2 (MuV^{JL2}) and Jeryl Lynn 5 (MuV^{JL5}) (2). Vaccination with a single subcutaneous dose containing 1,000 50% cell culture infective doses leads to seroconversion rates of 85% (7). Several countries have developed alternative MuV vaccines. For example, Leningrad-3, Leningrad-Zagreb, and Urabe AM9 were developed in the Soviet Union, Croatia, and Japan, respectively (47). Clinical studies indicated similar and in some cases higher rates of seroconversion and protective efficacy compared to Jeryl Lynn (5, 39, 44). Unlike the Jeryl Lynn vaccine, which is not associated with aseptic meningitis (6, 39), Leningrad-3, Leningrad-Zagreb, and Urabe AM9 have been shown to cause central nervous system (CNS) complications at unacceptably high rates in vaccinees (13, 19, 43).

The neurotrophic nature of MuV necessitates that vaccine lots be routinely tested to ensure sufficient neuroattenuation before release. World Health Organization (WHO) guidelines require MuV vaccines to be tested in macaque monkeys (47).

* Corresponding author. Mailing address: School of Biomedical Sciences, The Queen's University of Belfast, Belfast, BT9 7BL, Northern Ireland, United Kingdom. Phone: 44 28 9097 2060. Fax: 44 28 9097 5877. E-mail: p.duprex@qub.ac.uk.

▽ Published ahead of print on 2 May 2007.

Although the monkey neurovirulence test is widely used, its reliability has been questioned, since it has been reported that this test was unable to distinguish between different vaccines and cerebrospinal fluid isolates obtained from vaccinees with aseptic meningitis (1, 36). Thus, it has been desirable to develop alternative animal models for routine assessment of MuV neurovirulence. Attempts to develop a murine model of MuV neurovirulence have been unsuccessful, because newborn mice, infected intracerebrally with MuV^{KH}, MuV^{RW}, or MuV^{SBL-1} strains, showed no overt signs of disease, and virus was not recovered from brain samples (23). Encephalitis in the brains of newborn hamsters infected with rodent brain-adapted strains of MuV has been studied extensively (21). Both intracerebral inoculation and intraperitoneal inoculation with the MuV^{KH} strain lead to widespread CNS infection and mortality (21, 50). However, the hamster model is unable to discriminate between MuV strains with known differences in human neurovirulence; comparison of the neurovirulence of three strains of MuV revealed that the nonneurovirulent Jeryl Lynn vaccine was most similar to the rodent brain-adapted MuV^{KH} strain (51). Intracerebral infection of neonatal Lewis rats has been demonstrated to be a particularly sensitive indicator of the relative human neurovirulence of MuV strains (34). Intracerebral infection with 100 PFU of the MuV^{KH} strain led to extensive hydrocephalus of the lateral and third ventricles, whereas infection with the Jeryl Lynn vaccine strain did not. Further validation of the rat neurovirulence test (RNVT) with a range of MuV strains supports the suggestion that this model can accurately discriminate MuV strains with different levels of neurovirulence (35). In the RNVT, hydrocephalus of the lateral ventricle is measured and RNVT scores are calculated as the percentage (area) of the total brain section occupied by the lateral ventricle. RNVT scores parallel the clinical histories or attenuation status of isolates (35). The RNVT for the prediction of MuV neurovirulence may therefore represent a significant improvement over previous animal models in terms of both accuracy and clinical relevance.

In spite of extensive efforts, an understanding of the molecular basis of MuV neurovirulence remains elusive. Sequence analysis of clinical isolates has identified positions in the HN and SH genes that may be important in neurovirulence (3, 8, 42). In addition, neuroattenuation of clinical isolates and neuroadaptation of vaccine strains have identified mutations in the N, M, F, HN, and L genes, and these may be associated with either an increase or a decrease in neurovirulence (33). However, no single mutation or group of mutations has been definitively identified as being associated with a neurovirulent phenotype. The development of an MuV reverse genetics system (14) and a reliable animal model for the prediction of MuV human neurovirulence (35) enables such questions to be addressed directly. In this study we utilized an MuV reverse genetics system based on the MuV^{JL5} vaccine strain (14). The neurovirulence of recombinant viruses containing envelope genes from the MuV^{KH} strain was tested using the RNVT. This approach enabled the contribution of individual genes to neurovirulence to be assessed in isolation. Evidence is presented that the F gene of MuV contains the major determinants of neurovirulence.

MATERIALS AND METHODS

Viruses and cells. The MuV^{KH} rodent brain-adapted strain was obtained from Steven A. Rubin (Center for Biologics Evaluation and Research, Food and Drug Administration, Bethesda, MD). The virus had been passaged twice on Vero cells, and retention of the neurovirulent phenotype had been confirmed by intracerebral infection of Lewis rats (34). Modified vaccinia virus Ankara (MVA-T7) was grown as previously described (15). A549 and Vero cells were grown in Dulbecco's modified Eagle medium (Invitrogen) supplemented with 10% (vol/vol) fetal calf serum (Invitrogen). Cells were observed by phase-contrast microscopy using a DM IRBE inverted microscope (Leica Microsystems). Photomicrographs were obtained using a DC 300F digital camera connected to a computer running IM50 imaging software (Leica Microsystems).

Multistep growth analysis. Vero cells were cultured to 70% confluence in 35-mm-diameter petri dishes. Cells were infected at a multiplicity of infection (MOI) of 0.01 for 1 h at 37°C. The inoculum was removed and replaced with Optimem (Invitrogen). Samples were taken at 12 hourly intervals up to 72 h postinfection (hpi). Cells were scraped into the supernatant, and cell-associated virus was released by freeze-thawing the samples once. Titers were determined in triplicate by the 50% end point dilution assay as previously described (15).

Construction of an MuV expression cassette vector. The multiple cloning site (MCS) of the eukaryotic expression plasmid pCG (10) was modified to include restriction sites that are absent in the MuV^{JL5} full-length clone (pMuVFL). Digestion of pCG with BamHI and PstI removed the majority of the existing MCS. Two complementary oligonucleotides, priCG(MPBSH)+ (5′-GAT CCG ATA CAA CGC GTG ATA CAG TTT AAA CGA TAC ACA CGT CGA TAC AGC GAT CGC GAT ACA GTT AAC GAT ACA CTG CA-3′) and priCG(MPBSH)− (5′-GTG TAT CGT TAA CTG TAT CGC GAT CGC TGT ATC GAC GTG TGT ATC GTT TAA ACT GTA TCA CGC GTT GTA TCG-3′), were annealed as previously described (15) to produce an oligonucleotide linker containing MluI, PmeI, BtrI, SgfI, and HpaI restriction sites (underlined) separated by 6-bp spacers with BamHI- and PstI-compatible ends (Fig. 1A). This was ligated into the linearized vector to generate pCG(MPBSH).

Modification of the MuV full-length cDNA clone. The full-length MuV plasmid pMuVFL was sequentially modified by site-directed mutagenesis to include a number of unique restriction sites in the UTRs flanking the M, F, SH, and HN genes. An MluI site was introduced into the P 3′ UTR at position 3171 (numbered according to the full-length antigenomic sequence). Similarly, a PmeI site was introduced into the M 3′ UTR at position 4465, a BtrI site was introduced into the SH 5′ UTR at position 6248, and an SgfI site was introduced into the SH 3′ UTR at position 6470. In addition, a BstEII site at position 6929 (located in the HN open reading frame [ORF]) was silently ablated to facilitate cloning. The resulting plasmid was designated pMuV(MPBS) (Fig. 1B).

RNA preparation and RT-PCR. Total RNA was prepared using TRIzol solution as outlined by the manufacturer (Invitrogen). First-strand cDNA synthesis was performed on RNA (2 μg) using Moloney murine leukemia virus reverse transcriptase (RT) and gene-specific primers. PCRs were set up using 2% of the cDNA reaction as a template, MuV-specific primers that flank each of the four envelope-associated genes, and the proofreading DNA polymerase *Pfu* (New England Biolabs). Restriction sites (underlined) were introduced into the primers to facilitate cloning of the DNA fragments. A 1,294-bp insert encompassing the MuV^{KH} M gene was amplified using oligonucleotides priMuVMluI+ (5′-GAA TTC ACC AGG AGC ACC AGA CGC GTG GAA AAA TCT ATG AAC TGA G-3′) and priMuVMR (5′-TTC TAT AAG TTT AAA CGA ATT ACC ACC GGT CAA ATT TGC-3′), which contain MluI and PmeI sites, respectively. A 1,783-bp insert spanning the MuV^{KH} F gene was generated using oligonucleotides priMuVPmeI+ (5′-AAT TTG ACC GGT GGT AAT TCG TTT AAA CTT ATA GAA AAA ATA AGC CTA GAA G-3′) and priMuVBtrI− (5′-CGG CAT AGT GCG ACG GCA GGG TGA CGT GAC GTT ACG ACC CTA GGA GAT-3′), which contain PmeI and BtrI sites, respectively. A 222-bp insert encompassing the SH gene of MuV^{KH} was amplified using oligonucleotides priMuVBtrI+ (5′-ATC TCC TAG GGT CGT AAC GTC ACG TCA CCC TGC CGT CGC ACT ATG CCG-3′) and priMuVSgfI− (5′-TGC AGC TTG TTC TAG CGT GAG CGA TCG CGA CTT GTC CTA ATT GGG GAT-3′), which contain BtrI and SgfI sites, respectively. A 1,868-bp insert spanning the MuV^{KH} HN gene was amplified using priHNSgfI+ (5′-CAA GTC GCG ATC GCT CAC GCT AGA ACA AGC TG-3′) and priMuVHN− (5′-AAT CTG GCT AGC ACA GGT AGA ATT TGG AAT TC-3′), which contain SgfI and NheI, respectively.

Construction of eukaryotic M, F, SH, and HN protein expression vectors. Eight plasmids that express the MuV^{JL5} and MuV^{KH} envelope-associated genes were generated using pCG(MPBSH). The vector was cleaved with the appropriate two restriction enzymes to insert the M (MluI and PmeI), F (PmeI and

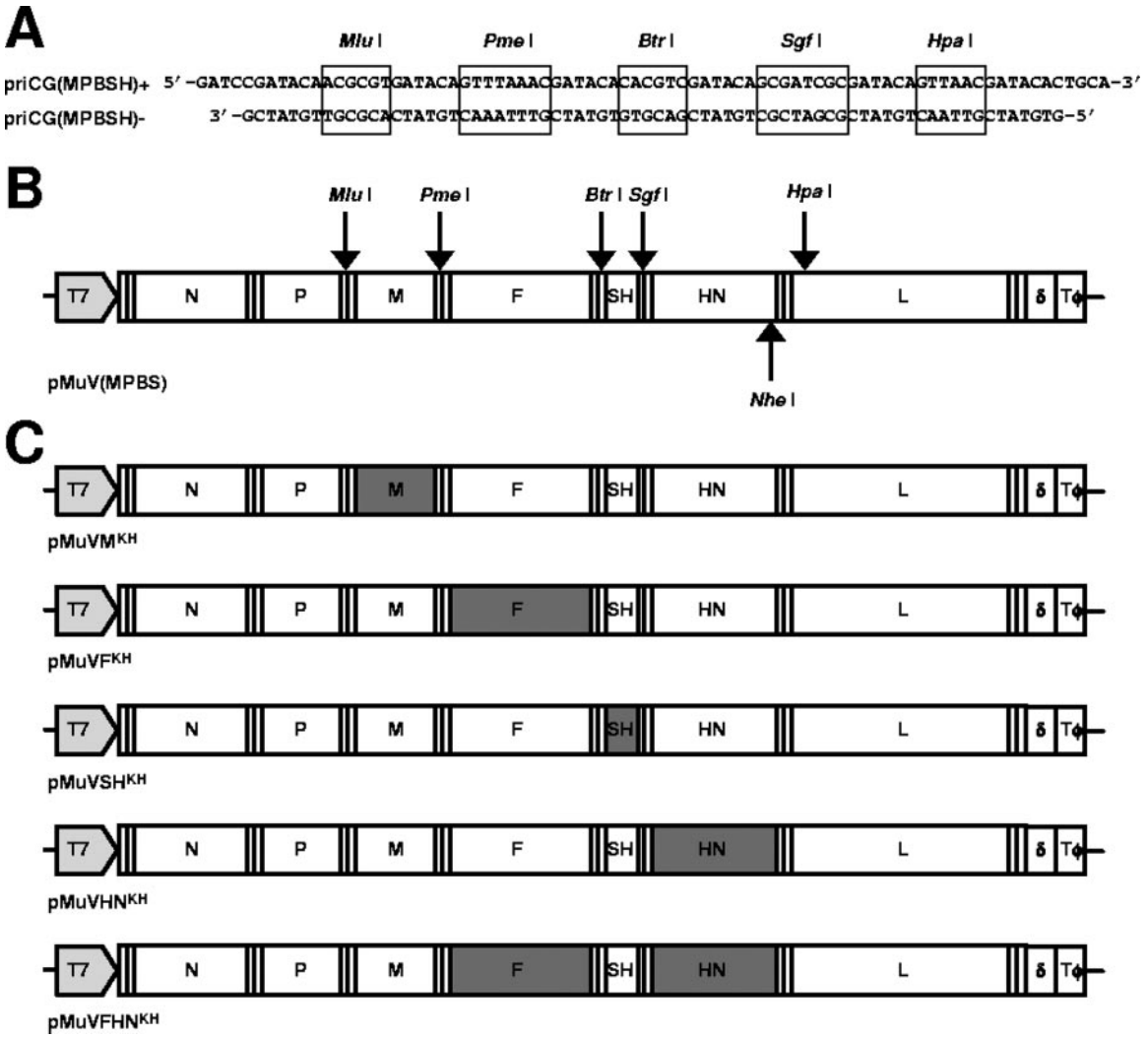

FIG. 1. Construction of a MuV expression vector and modification of the full-length infectious clone. (A) Complementary oligonucleotides were annealed to generate BamHI/PstI-compatible ends and inserted into a BamHI/PstI-cut pCG vector to introduce unique MluI, PmeI, BtrI, SgfI, and HpaI restriction sites. (B) The full-length MuV infectious clone pMuVFL was modified to introduce unique MluI, PmeI, BtrI, and SgfI restriction sites to generate pMuV(MPBS). (C) The M, F, SH, and HN genes from the MuV^{KH} strain were amplified by RT-PCR and inserted individually or in combination into pMuV(MPBS).

BtrI), SH (BtrI and SgfI), and HN (SgfI and HpaI) genes, which were generated either by RT-PCR from MuV^{KH} RNA or by restriction digestion of pMuV (MPBS). Thus, pCG(MPBS) cleaved with MluI and PmeI and ligated with the equivalently restricted MuV^{KH} M gene RT-PCR product generated $pCGMuVM^{KH}$, and pCG(MPBS) cleaved with MluI and PmeI and ligated with equivalently restricted pMuV(MPBS) generated $pCGMuVM^{JL5}$. Constructs expressing F ($pCGMuVF^{KH}$ and $pCGMuVF^{JL5}$), SH ($pCGMuVSH^{KH}$ and $pCGMuVSH^{JL5}$), and HN ($pCGMuVHN^{KH}$ and $pCGMuVHN^{JL5}$) were generated using similar approaches.

Sequence analysis of MuV^{KH} envelope-associated genes. No complete genomic consensus sequence for the MuV^{KH} strain of MuV is available. At least three independent clones were sequenced during construction of the MuV^{KH} expression vectors using primers specific for each gene. Sequences were assembled and compared using DNA sequence analysis software (DNAStar). Clones with consensus sequences were used for all subsequent manipulations.

Construction of full-length clones with MuV^{KH}-derived envelope-associated genes. Five plasmids that contain MuV^{KH} envelope-associated genes were generated in pMuV(MPBS). The plasmid was cleaved with the appropriate two restriction enzymes to insert the MuV^{KH} M (MluI and PmeI), F (PmeI and BtrI), SH (BtrI and SgfI), or HN (SgfI and NheI) gene from the pCG-based eukaryotic expression vectors. Thus, pMuV(MPBS) cleaved with MluI and PmeI and ligated with the equivalently restricted MuV^{KH} M gene generated $pMuVM^{KH}$. Constructs expressing F ($pMuVF^{KH}$), SH ($pMuVSH^{KH}$), and HN ($pMuVHN^{KH}$) were generated using similar approaches. The Kilham HN gene was inserted into SgfI- and NheI-restricted $pMuVF^{KH}$ to generate $pMuVFHN^{KH}$, which contained both MuV^{KH} glycoproteins.

Rescue of recombinant viruses from cDNA. A549 cells, grown to 40% confluence in 35-mm-diameter petri dishes, were infected with MVA-T7 at an MOI of 0.5. Transfections were carried out essentially as outlined previously (14). Plasmids pMuV-N (300 ng), pMuV-P (50 ng), and pMuV-L (200 ng) and the plasmids containing copies of the full-length antigenomes (6 μg) were transfected into the cells over 24 h. After this time, the transfection mixtures were removed and replaced with growth medium, and the cells were incubated for a further 24 h. Vero cells (~300,000) were added to each well, and monolayers were observed for as long as 10 days for the appearance of cytopathic effect. Recombinant viruses were plaque purified once in Vero cells and passaged four times to generate working stocks.

Indirect immunofluorescence and confocal scanning laser microscopy. Vero cells were grown on glass coverslips in 35-mm-diameter petri dishes to 90% confluence. Cells were infected/transfected, fixed, processed, and mounted as previously described (16). A primary anti-MuV F monoclonal antibody (5.418) was used at a dilution of 1:500 (30). A fluorescein isothiocyanate-conjugated

secondary antibody (DAKO) was used at a dilution of 1:100. A Leica TCS SP2 Acousto-Optical Beam Splitter confocal scanning laser microscope, equipped with HeNe lasers as the source for the ion beam, was used to examine the samples for fluorescence as previously described (16).

Assessment of neurovirulence. One-day-old suckling Lewis rats were obtained from in-house breeding colonies in the Laboratory Service Unit, The Queen's University, Belfast, United Kingdom. Rats were inoculated with 100 tissue culture infective doses ($TCID_{50}$) of the viruses in the right parietal area of the skull, approximately 1 mm right of the midline and midway between the eye and the ear under mild isoflurane anesthesia (10 μl). Fourteen to 50 animals per virus were infected. Animals were monitored daily for signs of disease, and individuals were sacrificed by isoflurane narcosis between 3 and 30 days postinfection (dpi). All experimentation was carried out under appropriate animal licenses regulated by the Home Office. Whole brains were removed and immersed in 10% (vol/vol) buffered formalin. Brains were blocked into right and left hemispheres, processed, and embedded in paraffin wax. Whole brains from animals at 3 dpi were homogenized in Optimem (3 ml), and virus was recovered following a single freeze-thawing. Homogenized samples were centrifuged at 4,000 × *g* for 5 min. Clarified supernatant was added to Vero cells grown to a confluence of 70% in 35-mm-diameter petri dishes. Total RNA was prepared from the cell pellet using TRIzol solution. RT-PCRs were set up using total RNA (1 μg), MuV-specific primers $priMuV^{JL5}3993+$ (5′-GGT TCC ACC TAT GTA ATC TG-3′) and $priMuV^{JL5}4681-$ (5′-CTT GAC TAC TAC GTA GGA GC-3′), and a *Reverse*-iT one-step kit (ABgene).

Pathological and immunohistochemical assessment. Microtome-cut sections (thickness, 7 μm) were taken at a distance of 200 μm from the midline of the paraffin-embedded tissue (16). Sections were dewaxed, and after microwave antigen retrieval, a monoclonal antibody that recognizes the N protein of MuV (N93-51/01) was used for immunohistochemistry at a dilution of 1:4,000. Specific binding sites were immunodetected as previously described (38).

Hematoxylin and eosin-stained brain sections were digitized using a ScanScope slide scanner (Aperio Technologies) and viewed using an Imagescope (version 5.00) virtual slide viewing software package (Aperio Technologies). Sections were viewed at equivalent magnifications, and a snapshot was exported as a tagged image format file. These were further analyzed using ImageJ 1.33u image processing and analysis software (National Institutes of Health). Regions of interest (ROI) were selected using a polygon selection tool. The entire brain section, excluding the cerebellum and olfactory bulb, was selected (ROI 1), and the area was determined in pixels. The lateral ventricle was selected (ROI 2), and the area was determined in pixels. The extent of hydrocephalus (RNVT score) was expressed as the percentage of the total brain section occupied by the lateral ventricle, i.e., (ROI 2/ROI 1) × 100.

Nucleotide sequence accession numbers. Sequences of MuV^{KH} envelope-associated genes have been submitted to GenBank under accession numbers EF493023 (M), EF493024 (F), EF493025 (SH), and EF493026 (HN).

RESULTS

Generation of constructs expressing MuV envelope-associated genes. The goal of this study was to determine if the envelope-associated proteins of the MuV^{KH} strain were capable of conferring a neurovirulent phenotype on a nonneurovirulent vaccine strain and, if so, which genes were required. Sequences of the UTRs flanking each of the genes were examined for areas that could be altered to restriction sites absent in the MuV^{JL5} full-length clone. Regions outside the consensus GS and GE signals were chosen, and four sites (MluI, PmeI, BtrI, and SgfI) that flanked M, F, and SH were introduced (Fig. 1B). These sites introduce either 2 or 3 nucleotide changes into the UTRs, resulting in a total of 12 nucleotide changes from the MuV^{JL5} consensus. Endogenous restriction sites (NheI and HpaI) at the 3′ end of the HN ORF and the 5′ end of the L ORF were used in combination with the SgfI site to facilitate the cloning of HN ORFs. The MCS of a eukaryotic expression plasmid was modified to include these sites using synthetic oligonucleotides (Fig. 1A). This plasmid, pCG (MPBSH), was used as the cloning vector for the MuV^{KH} envelope-associated genes (M, F, SH, and HN) following RT-PCR using primers that contain these sites. An equivalent complementary set of constructs was generated to express MuV^{JL5} proteins.

TABLE 1. Amino acid differences in the M, F, SH, and HN proteins of MuV^{JL5} and MuV^{KH}

Amino acid sequence[a] in:			
M (375 aa)	F (538 aa)	SH (57 aa)	HN (582 aa)
Y140H	N2K	V14L	I44T
I207V	Y11F	Y34H	S69F
M274I	T24I	A37T	I135V
R373S	L95P	H55Q	A218V
	S177N		I279T
	Y290H		T288K
	M331I		L297F
	T431A		L336S
	F477V		Q354S
	G480S		Y442S
	S489A		H464N
			I473T
			R490S

[a] Lefthand residues belong to MuV^{JL5}; righthand residues belong to MuV^{KH}.

No complete genomic consensus sequence for the MuV^{KH} strain of MuV is available. In this study we focused on the envelope-associated proteins to determine if these contained residues that governed neurovirulence. Consensus sequences of the M, F, SH, and HN genes from a phenotypically neurovirulent MuV^{KH} strain were obtained. Partial and complete sequences of the MuV^{KH} F (AF143392), SH (X63706), and HN (AY502062) genes are available, whereas the sequence of M is unknown. Comparison with the published MuV^{KH} F sequence revealed a single amino acid coding change (F 36 W→R). Alignment of all available MuV F sequences shows that R is highly conserved at this position. Comparison with the published MuV^{KH} SH sequence revealed two amino acid coding changes (SH 33 T→N and SH 34 Y→H). An alignment of SH sequences of genotypes A to J shows that all genotype A strains, except for the previously published MuV^{KH}, encode SH 33 N 34 H (41). Surprisingly, 11 amino acid residues differed between our HN and the previously published sequence. At five of these positions (176, 385, 389, 447, and 523) our sequence predicted the highly (>95%) or totally conserved amino acid in an alignment of all 69 complete HN sequences available on GenBank. At three positions (372, 473, and 474), two amino acids were given in the alignment, with our sequence predicting one and the previously published sequence predicting the other amino acid. Positions 354 and 356 are variable in the alignment, whereas at position 297 we predicted a phenylalanine instead of the conserved leucine found in other sequences. Amino acid differences between our MuV^{KH} and MuV^{JL5} are summarized in Table 1. The UTRs of MuV^{KH} and MuV^{JL5} differed at a limited number of positions. The F gene 3′ and 5′ UTRs each contained four nucleotide differences, whereas the 3′ and 5′ UTRs of the HN gene contained two nucleotide differences each. The SH gene 3′ UTR contained one nucleotide difference, and the 5′ UTR contained two. The UTRs of the M gene did not contain any nucleotide differences.

MuV^{JL5} and MuV^{KH} glycoproteins function heterologously. Expression of MuV F and HN in transfected cells induces

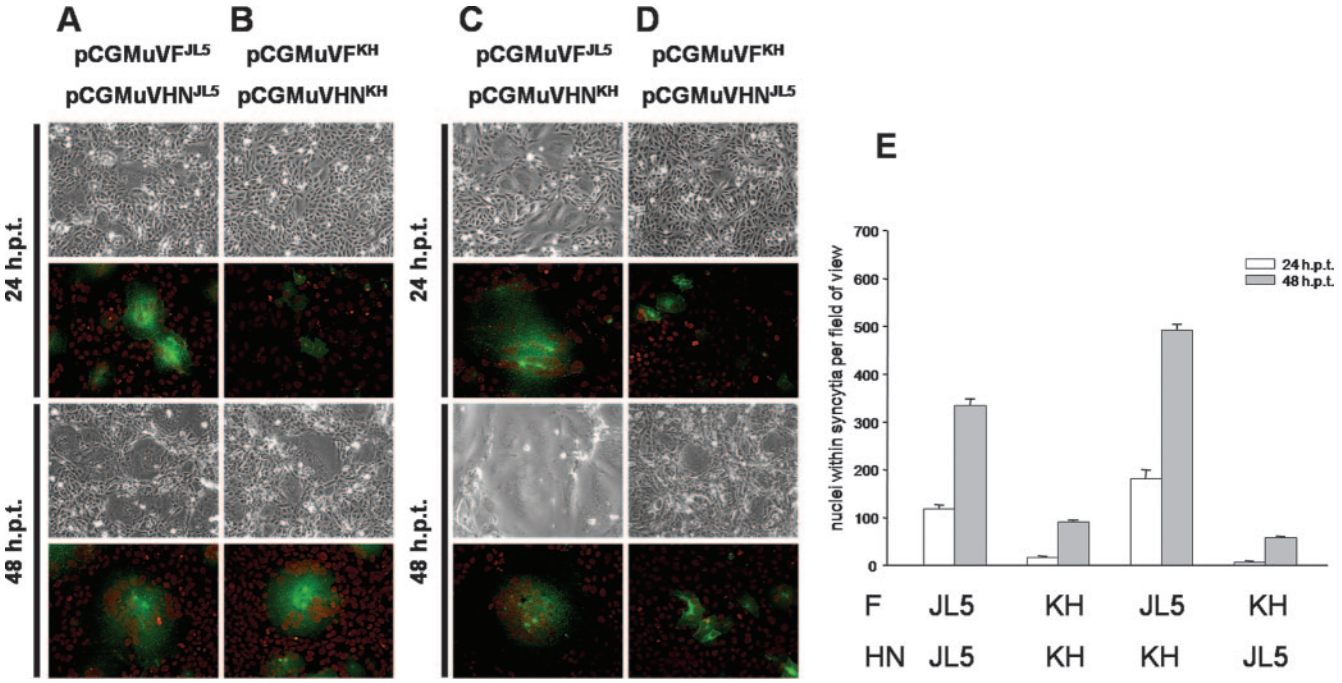

FIG. 2. Analysis of MuV fusion in transiently transfected cells. Vero cells were transfected with pCGMuVF^{JL5} (1 μg) and pCGMuVHN^{JL5} (1 μg) (A), pCGMuVF^{KH} (1 μg) and pCGMuVHN^{KH} (1 μg) (B), pCGMuVF^{JL5} (1 μg) and pCGMuVHN^{KH} (1 μg) (C), or pCGMuVF^{KH} (1 μg) and pCGMuVHN^{JL5} (1 μg) (D). Phase-contrast images were taken 24 and 48 hpt. Equivalent transfections were performed on Vero cells grown on glass coverslips. At 24 and 48 hpt, cells were fixed and immunocytochemistry was performed using a primary anti-MuV F monoclonal antibody (5.418) at a dilution of 1:500 and a fluorescein isothiocyanate-conjugated secondary antibody at a dilution of 1:100. Nuclei were counterstained using propidium iodide. (E) Fusion was quantified by counting the number of cell nuclei involved in syncytia in 20 randomly chosen fields of view.

syncytia (40). Constructs derived from MuV^{KH} and MuV^{JL5} were transfected into Vero cells to determine if homologous and heterologous pairs of MuV glycoproteins could cooperate to give fusion. Neither F nor HN formed syncytia in isolation (data not shown), and transfection with homologous plasmids resulted in the formation of syncytia 24 h posttransfection (hpt) (Fig. 2A and B). Cell fusion was quantified by counting the number of nuclei contained within syncytia in 20 randomly chosen fields of view. Coexpression of MuV^{JL5} F and HN produced higher levels of fusion than coexpression of MuV^{KH} F and HN (Fig. 2E). Transient transfection of heterologous sets of glycoprotein expression vectors from each strain indicated that the glycoproteins complemented one another and formed functional fusion complexes (Fig. 2C and D). Surprisingly, expression of MuV^{JL5} F with MuV^{KH} HN resulted in a significant increase in the level of cell fusion, and the monolayer was extensively fused within 48 h (Fig. 2C). In contrast, expression of MuV^{KH} F with MuV^{JL5} HN resulted in very limited cell fusion (Fig. 2D). Quantification of cell fusion confirmed that expression of MuV^{JL5} F with MuV^{KH} HN produced higher levels of fusion than either of the homologous glycoprotein combinations, whereas expression of MuV^{KH} F with MuV^{JL5} HN produced lower levels than either of the homologous glycoprotein combinations (Fig. 2E). Taken together, these data indicated that the glycoproteins from both MuV^{JL5} and MuV^{KH} could form functional fusion complexes even when heterologous combinations were expressed and suggested that recombinant viruses containing such combinations may be viable.

Generation of recombinant viruses expressing the envelope-associated genes from MuV^{KH}. A series of full-length plasmids that contained individual MuV^{KH} envelope-associated genes were constructed (Fig. 1C). In addition, a clone (pMuVFHN^{KH}) containing both viral glycoproteins was constructed. A rescue system based on pMuV(MPBS) was employed to generate recombinant viruses from each construct. The recombinant viruses were used to infect Vero cells at an MOI of 0.01, and the level of cell-to-cell fusion was recorded after 24 and 48 h. All viruses induced syncytia in Vero cells to a lesser or greater extent (Fig. 3). The parental virus, rMuV^{MPBS}, produced syncytia composed of 30 to 60 nuclei at 48 hpi. Recombinant viruses containing the MuV^{KH} M or SH gene were indistinguishable from rMuV^{MPBS}. The MuV^{KH} strain was less fusogenic, and syncytia comprised only 10 to 30 nuclei after 48 h and were not visible at 24 hpi. Recombinant viruses containing the MuV^{KH} F gene either alone or in combination with the MuV^{KH} HN gene were indistinguishable from MuV^{KH}; no fusion was visible at 24 hpi, and at 48 hpi, small syncytia containing 10 to 30 nuclei were observed. A recombinant virus containing the MuV^{KH} HN gene produced extensive cell-to-cell fusion at 24 hpi; this progressed to encompass the entire monolayer after 48 h. Therefore, recombinant viruses expressing homologous or heterologous glycoprotein combinations had fusion phenotypes that closely paralleled those seen in transient expression experiments.

Multistep growth analysis was performed to compare the growth of the recombinant viruses. Most viruses had similar growth kinetics and achieved titers of approximately $10^{5.5}$

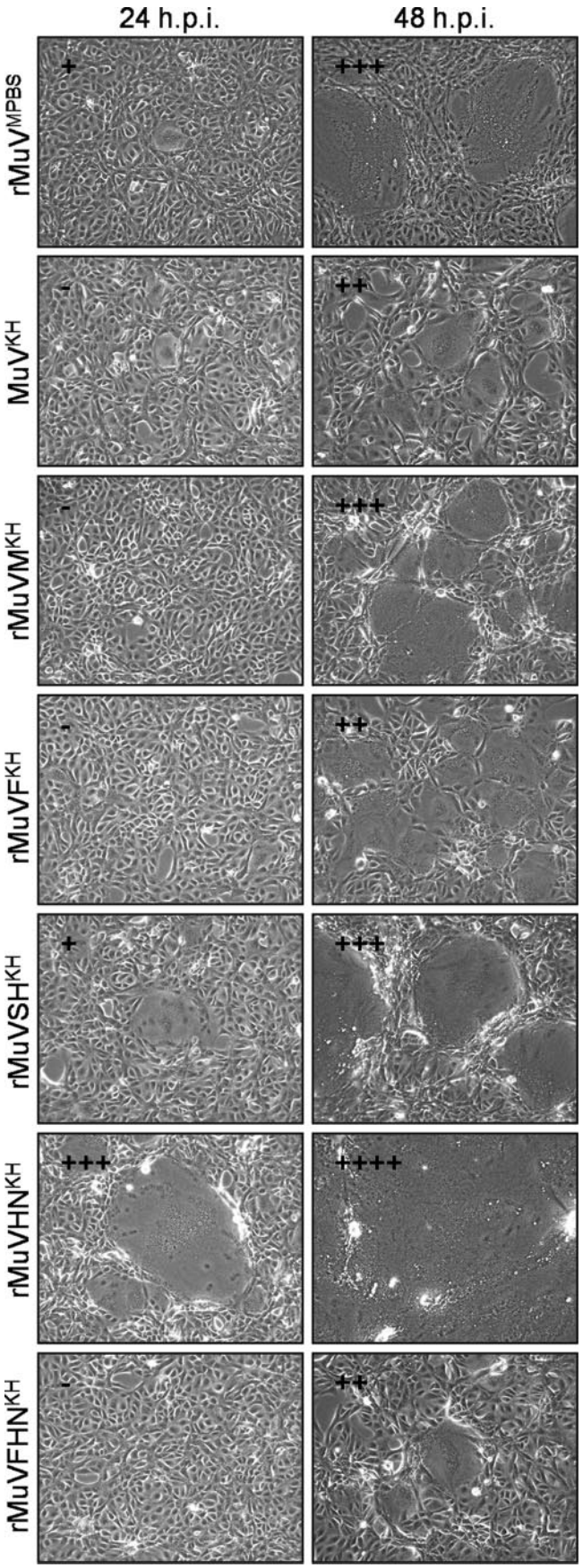

FIG. 3. Syncytia produced by recombinant viruses on Vero cells. Vero cells were infected with each of the recombinant viruses at an MOI of 0.01. Phase-contrast images were taken 24 and 48 hpi. Semiquantitative scoring of cell fusion was performed based on the average number of nuclei contained within individual syncytia: −, no fusion; +, <10 nuclei per syncytium; ++, 10 to 30 nuclei per syncytium; +++, 30 to 60 nuclei per syncytium; ++++, complete fusion of the monolayer.

$TCID_{50}$/ml at 60 hpi (Fig. 4). The MuV^{KH} strain and the recombinant virus $rMuVF^{KH}$ grew to higher titers of approximately 10^7 at 60 hpi. The recombinant virus $rMuVM^{KH}$ achieved a titer of approximately $10^{6.5}$ $TCID_{50}$/ml at 60 hpi. These data indicated that the introduction of nonhomologous genes into $rMuV^{MPBS}$ had no adverse effect on the growth of the recombinant viruses.

The F gene of MuV^{KH} is a major determinant of neurovirulence. The severity of hydrocephalus following intracerebral inoculation of neonatal Lewis rats with MuV has been shown previously to correlate with the known human neurovirulence of various MuV isolates (35). This model was utilized to assess the neurovirulence phenotypes of each of the recombinant viruses. One-day-old Lewis rats (*n*, 14 to 50) were inoculated intracerebrally with 100 $TCID_{50}$ of each virus. At 30 dpi, rats were euthanized and the severity of hydrocephalus (RNVT score) was determined as the percentage of the brain cross-section occupied by the lateral ventricle. Representative cross-sections for each virus infection are shown in Fig. 5A. Few animals infected with the parental $rMuV^{MPBS}$ virus developed hydrocephalus, whereas extensive dilation of the lateral ventricle was observed in many animals infected with MuV^{KH} (Fig. 5B). Not all animals infected with MuV^{KH} developed hydrocephalus. However, all data points were included in the analysis. The average severity of hydrocephalus was determined as 0.8% ± 0.3% for $rMuV^{MPBS}$ versus 12.7% ± 1.3% for MuV^{KH}. Recombinant viruses based on $rMuV^{MPBS}$ containing genes from MuV^{KH} were also examined. Viruses containing the MuV^{KH} M, SH, or HN gene in isolation failed to induce significant hydrocephalus, whereas a virus that contained the MuV^{KH} F gene induced severe hydrocephalus in many animals (8.4% ± 1.1%). A virus containing both the MuV^{KH} glycoproteins induced a marginally higher level of hydrocephalus (10.5% ± 2.1%), although this was not statistically different from the level for the MuV^{KH} F-containing virus in an unpaired Student *t* test ($P = 0.36$).

Infection of neonatal Lewis rats was confirmed by both RT-PCR and isolation of virus from the brain tissue of a single animal from each virus group at 3 dpi (data not shown). Viral titers were highest for those viruses which induced hydrocephalus, with $rMuVF^{KH}$, $rMuVFHN^{KH}$, and MuV^{KH} reaching titers of $10^{2.2}$, $10^{4.5}$, and $10^{6.0}$ $TCID_{50}$/g of brain tissue, respectively. Detection of MuV N antigen in brain sections of animals at 3 dpi was also performed for a limited number of animals infected with $rMuV^{MPBS}$, $rMuVF^{KH}$, $rMuVHN^{KH}$, and $rMuVFHN^{KH}$, since these viruses induced hydrocephalus to a lesser or greater extent (Fig. 6). Antigen-positive cells were detected for each virus examined. Infection was restricted to the ependymal cells, which line the ventricular system. Fewer antigen-positive cells were observed in brain sections from

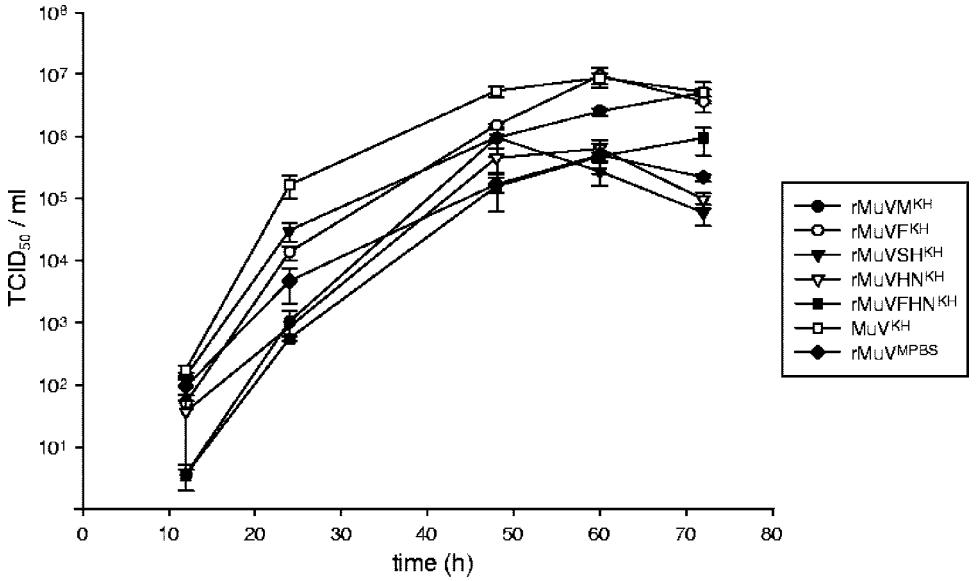

FIG. 4. Growth kinetics of the recombinant viruses. Vero cells were infected at an MOI of 0.01. Samples were taken at regular intervals up to 72 hpi. Cells were scraped into the supernatant and cell-associated virus released by freeze-thawing the samples once. Titers were determined in triplicate by the 50% end point dilution assay.

animals infected with those viruses that did not induce hydrocephalus (i.e., rMuV^{MPBS} and rMuVHN^{KH}) compared to those viruses that did induce hydrocephalus (i.e., rMuVF^{KH} and rMuVFHN^{KH}).

DISCUSSION

The identification of molecular markers of MuV neurovirulence has been hampered in large part by the lack of a suitable small-animal model capable of reliably predicting the potential neurovirulence of virus strains. The development of the RNVT represents a significant improvement over previous models and, in combination with the MuV rescue system, has enabled the current study to be carried out.

Recently another group published a sequence for the MuV^{KH} HN gene (32). Comparison of this sequence with that derived in this study revealed a total of 11 amino acid differences. The HN sequence determined here was derived directly from a stock of MuV^{KH} that was shown to be neurovirulent in rats. The phenotype of the MuV^{KH} strain used in the other study was not investigated, and thus whether the differences would render it nonpathogenic is unknown. The protein of the strain used in this study was able to induce syncytia in transiently transfected cells when coexpressed with both homologous and heterologous F proteins. A recombinant virus that expressed only MuV^{KH} HN was viable and grew to titers of approximately $10^{5.5}$ $TCID_{50}$/ml. Furthermore, a recombinant virus that expressed both HN and F from our MuV^{KH} was able to induce hydrocephalus in rat brains to a similar degree as MuV^{KH}. However, in light of these sequence differences, further work will be needed in order to clarify the contribution of MuV^{KH} HN to neurovirulence. To date, most studies of the role of specific mutations in MuV neurovirulence have concentrated on the HN protein. Growth of MuV^{KH} in the presence of a monoclonal antibody known to inhibit the hemagglutination of human erythrocytes resulted in the isolation of several mutants with increased neuraminidase activity (24). One of the mutants (M13) was found to have reduced neurovirulence in hamsters following intracerebral inoculation compared to the parental MuV^{KH} strain. Analysis of infected brains by immunohistochemistry revealed that MuV^{KH}-infected animals had widespread infection of the CNS involving both ependymal cells and neurons. In contrast, the viral antigen in M13-inoculated animals was largely restricted to ependymal cells, with only isolated neurons infected. In a subsequent study, the HN genes, but not the other envelope components, of the antibody escape mutants were sequenced (22). Mutant M13 was found to contain a single nonconservative mutation (HN 360 R→C), indicating that HN plays an important role in neurovirulence. Sequence analysis of the Urabe AM9 component of the Trivirix measles, mumps, and rubella vaccine produced by Smith, Kline & French with cerebrospinal fluid isolates from postvaccination meningitis cases revealed that the vaccine is actually a mixture of at least two strains of virus that differ at amino acid 335 (8). Postvaccination meningitis appears to result from selection of the HN K335 variants. However, a subsequent study was unable to find a correlation of HN K335 with postvaccination complications (4). The Jeryl Lynn vaccine, which is not associated with high rates of postvaccination meningitis, also contains K335 in the HN proteins of both the MuV^{JL2} and MuV^{JL5} components, indicating that this single amino acid is not sufficient to confer a neurovirulent phenotype (28). These inconsistencies in the suggested link of genotype and phenotype suggest that there are other mutations elsewhere in the genome that play a key role in neurovirulence.

In contrast to earlier studies, the ability to generate recombinant MuV that can be assessed in a reliable animal model has enabled the contribution of individual genes to neurovirulence to be investigated. The MuV^{JL5} and MuV^{KH} strains

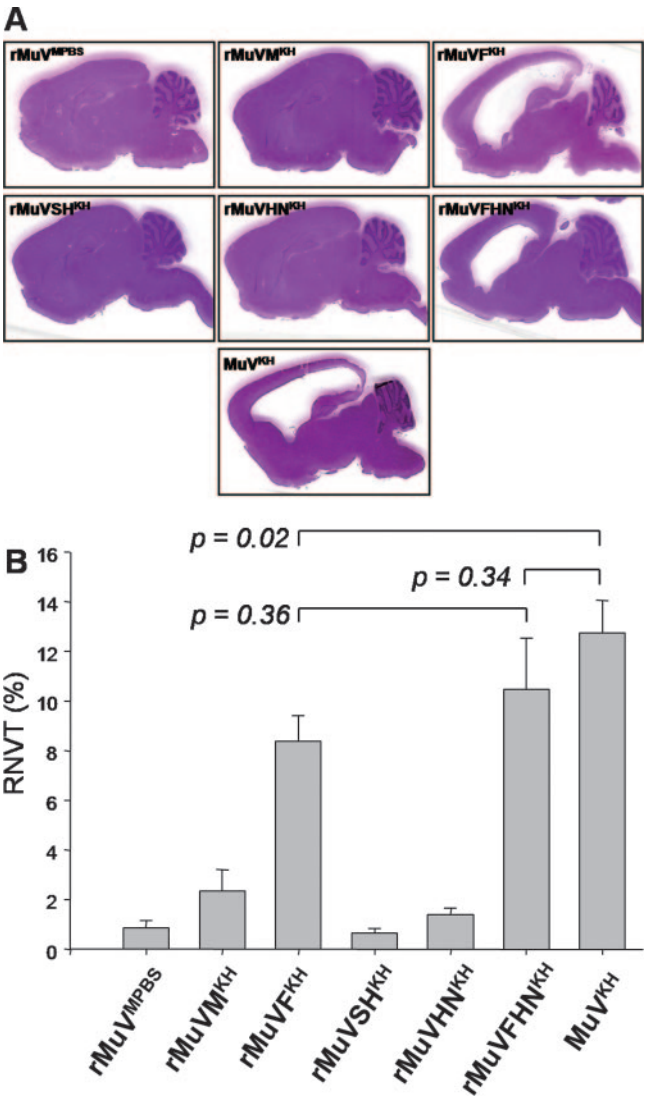

FIG. 5. Assessment of neurovirulence of the recombinant viruses in rats. One-day-old Lewis rats were inoculated intracerebrally with 100 $TCID_{50}$ of $rMuV^{MPBS}$ ($n = 21$), $rMuVM^{KH}$ ($n = 24$), $rMuVF^{KH}$ ($n = 50$), $rMuVSH^{KH}$ ($n = 19$), $rMuVHN^{KH}$ ($n = 24$), $rMuVFHN^{KH}$ ($n = 14$), or MuV^{KH} ($n = 22$). Animals were sacrificed 30 dpi, and whole brains were removed, blocked into right and left hemispheres, processed, and embedded in paraffin wax. Microtome-cut sections (7 μm) were taken at a distance of 200 μm from the midline of the paraffin-embedded tissue and stained with hematoxylin and eosin. (A) Representative sections from animals infected with each of the recombinant viruses. (B) Sections were digitized, and the extent of hydrocephalus (RNVT score) was expressed as the percentage of the total brain section occupied by the lateral ventricle.

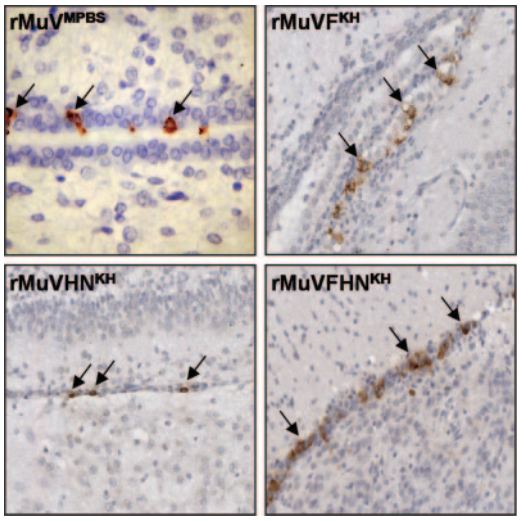

FIG. 6. Immunohistochemical assessment. One-day-old Lewis rats were inoculated intracerebrally with 100 $TCID_{50}$ of $rMuV^{MPBS}$, $rMuVF^{KH}$, $rMuVHN^{KH}$, or $rMuVFHN^{KH}$. Animals were sacrificed 3 dpi, and whole brains were removed, processed, and sectioned. A monoclonal antibody that recognizes the N protein of MuV (N93-51/01) was used for immunohistochemistry at a dilution of 1:4,000. Representative sections show infected cells (arrows) in regions lining the lateral ventricle.

represent two extremes of MuV neurovirulence in this model. MuV^{KH} induces significant hydrocephalus, whereas MuV^{JL5} does not. Recombinant viruses that contained individual MuV^{KH} genes in a MuV^{JL5} background were generated. Expression of the MuV^{KH} F gene was sufficient to confer a neurovirulent phenotype. Previous studies have indicated that the F protein may be important for MuV neurovirulence. Neuroattenuation of the highly neurovirulent wild-type strain 88-1961 by passage in chicken embryo fibroblasts (CEF) resulted in a variant with decreased neurovirulence in rats (33). The neuroattenuated 88-1961 variant (88-1961-CEF) contained single-amino-acid substitutions in the F, HN, and L proteins. Amino acid 91 of the F protein, which is a heterogeneous mixture of proline and threonine in the parental stock, became homogeneous for threonine, which is part of a potential N-linked glycosylation site. Later studies by the same group support the suggestion that neurovirulence is associated with changes in the level of genetic heterogeneity at specific sites (37). Neuroattenuation of the Urabe AM9 strain on CEF and Vero cells was accompanied by changes in heterogeneity at several positions. The F gene contained four positions that either lost or gained heterogeneity (amino acids 120, 290, 370, and 393). It is noteworthy that position 290 is one of the nine positions where the F genes of MuV^{KH} and MuV^{JL5} differ.

For paramyxoviruses such as Newcastle disease virus, the capacity of the host cell to proteolytically cleave the F_0 protein correlates directly with virulence (29). However, the inability of some MuV strains to induce cell-to-cell fusion is not a result of uncleaved precursor F protein (26). The neuraminidase activity of the HN protein is an important factor in MuV cell-to-cell fusion (27). Strains with high neuraminidase activity, as determined by the hydrolysis of fetuin, cause no cell fusion, whereas strains with low neuraminidase activity cause extensive fusion. This observation is thought to be a consequence of the prolonged association of progeny virus with the plasma membrane of adjacent cells, resulting in increased cell-to-cell fusion. Strains with high neuraminidase activity are associated with the plasma membrane for a much shorter duration and so are less likely to induce cell-to-cell fusion. Studies on influenza virus have demonstrated that strains with low neuraminidase activity are more fusogenic (12) and are more pathogenic in mice (25). For MuV, the relationship between

fusion in vitro and virulence in both humans and animal models is less well understood. In one study, the nonfusing RW strain of MuV was grown in the presence of the competitive inhibitor of sialidase, 2-deoxy-2,3-dehydro-*N*-acetylneuraminic acid (DANA), and a sialidase-deficient variant that caused extensive syncytium formation in cell culture was obtained (45). Sequence data revealed two mutations in the fusing variant, HN 181 I→T and HN 261 G→K. However, intracerebral inoculation of neonatal hamsters with this variant produced an infection that the author described as indistinguishable from the nonfusing parental form (49). This suggests that there is no direct association between increased fusogenicity and neurovirulence. Moreover, in the current study, recombinant viruses that were more fusogenic, such as rMuV^{MPBS} and rMuVHN^{KH}, did not induce hydrocephalus, whereas those viruses that were less fusogenic, such as rMuVF^{KH} and rMuVFHN^{KH}, produced extensive hydrocephalus. Further work is therefore required to elucidate the mechanism whereby the MuV F protein modulates neurovirulence. Since the F proteins of MuV^{JL5} and MuV^{KH} differ at a limited number of positions, the generation of recombinant viruses containing individual mutations in isolation will allow the contribution of each of these to neurovirulence to be assessed. It will also be of interest to determine if the N, P, and L genes of MuV^{KH} contain determinants of neurovirulence by generating recombinant viruses expressing these in isolation or as a complex. Furthermore, the generation of recombinant viruses expressing genes from viruses known to be neurovirulent in humans, such as Urabe AM9, will be necessary to confirm that the MuV F gene is a major determinant of human neurovirulence.

ACKNOWLEDGMENTS

We are very grateful to David Clarke, Steve Udem (now at IAVI, New York, NY), and their colleagues at Wyeth (Pearl River, NY) for providing the reagents and protocols necessary to establish the basic rescue system for the Jeryl Lynn strain of mumps virus in our laboratory.

This work was supported by the Wellcome Trust (grant 064263).

REFERENCES

1. **Afzal, M. A., S. A. Marsden, R. M. Hull, P. A. Pipkin, M. L. Bentley, and P. D. Minor.** 1999. Evaluation of the neurovirulence test for mumps vaccines. Biologicals **27:**43–49.
2. **Afzal, M. A., A. R. Pickford, T. Forsey, A. B. Heath, and P. D. Minor.** 1993. The Jeryl Lynn vaccine strain of mumps virus is a mixture of two distinct isolates. J. Gen. Virol. **74:**917–920.
3. **Afzal, M. A., P. J. Yates, and P. D. Minor.** 1998. Nucleotide sequence at position 1081 of the hemagglutinin-neuraminidase gene in the mumps Urabe vaccine strain. J. Infect. Dis. **177:**265–266.
4. **Amexis, G., N. Fineschi, and K. Chumakov.** 2001. Correlation of genetic variability with safety of mumps vaccine Urabe AM9 strain. Virology **287:**234–241.
5. **Beck, M., R. Welsz-Malecek, M. Mesko-Prejac, V. Radman, M. Juzbasic, M. Rajninger-Miholic, M. Prislin-Musklic, V. Dobrovsak-Sourek, S. Smerdel, and D. W. Stainer.** 1989. Mumps vaccine L-Zagreb, prepared in chick fibroblasts. I. Production and field trials. J. Biol. Stand. **17:**85–90.
6. **Black, S., H. Shinefield, P. Ray, E. Lewis, R. Chen, J. Glasser, S. Hadler, J. Hardy, P. Rhodes, E. Swint, R. Davis, R. Thompson, J. Mullooly, M. Marcy, C. Vadheim, J. Ward, S. Rastogi, and R. Wise.** 1997. Risk of hospitalization because of aseptic meningitis after measles-mumps-rubella vaccination in one- to two-year-old children: an analysis of the Vaccine Safety Datalink (VSD) Project. Pediatr. Infect. Dis. J. **16:**500–503.
7. **Boulianne, N., G. De Serres, S. Ratnam, B. J. Ward, J. R. Joly, and B. Duval.** 1995. Measles, mumps, and rubella antibodies in children 5–6 years after immunization: effect of vaccine type and age at vaccination. Vaccine **13:**1611–1616.
8. **Brown, E. G., K. Dimock, and K. E. Wright.** 1996. The Urabe AM9 mumps vaccine is a mixture of viruses differing at amino acid 335 of the hemagglutinin-neuraminidase gene with one form associated with disease. J. Infect. Dis. **174:**619–622.
9. **Buynak, E. B., and M. R. Hilleman.** 1966. Live attenuated mumps virus vaccine. 1. Vaccine development. Proc. Soc. Exp. Biol. Med. **123:**768–775.
10. **Cathomen, T., C. J. Buchholz, P. Spielhofer, and R. Cattaneo.** 1995. Preferential initiation at the second AUG of the measles virus F mRNA: a role for the long untranslated region. Virology **214:**628–632.
11. **Centers for Disease Control and Prevention (CDC).** 2006. Mumps epidemic—United Kingdom, 2004–2005. Morb. Mortal. Wkly. Rep. **55:**173–175.
12. **Choppin, P. W.** 1963. Multiplication of two kinds of influenza A2 virus particles in monkey kidney cells. Virology **21:**342–352.
13. **Cizman, M., M. Mozetic, R. Radescek-Rakar, D. Pleterski-Rigler, and M. Susec-Michieli.** 1989. Aseptic meningitis after vaccination against measles and mumps. Pediatr. Infect. Dis. J. **8:**302–308.
14. **Clarke, D. K., M. S. Sidhu, J. E. Johnson, and S. A. Udem.** 2000. Rescue of mumps virus from cDNA. J. Virol. **74:**4831–4838.
15. **Duprex, W. P., I. Duffy, S. McQuaid, L. Hamill, S. L. Cosby, M. A. Billeter, J. Schneider-Schaulies, V. ter Meulen, and B. K. Rima.** 1999. The H gene of rodent brain-adapted measles virus confers neurovirulence to the Edmonston vaccine strain. J. Virol. **73:**6916–6922.
16. **Duprex, W. P., S. McQuaid, L. Hangartner, M. A. Billeter, and B. K. Rima.** 1999. Observation of measles virus cell-to-cell spread in astrocytoma cells by using a green fluorescent protein-expressing recombinant virus. J. Virol. **73:**9568–9575.
17. **Elango, N., T. M. Varsanyi, J. Kovamees, and E. Norrby.** 1988. Molecular cloning and characterization of six genes, determination of gene order and intergenic sequences and leader sequence of mumps virus. J. Gen. Virol. **69:**2893–2900.
18. **Enders, J. F.** 1946. Techniques of laboratory diagnosis, tests for susceptibility and experiments on specific prophylaxis. J. Pediatr. **29:**129–142.
19. **Furesz, J., and G. Contreras.** 1990. Vaccine-related mumps meningitis—Canada. Can. Dis. Wkly. Rep. **16:**253–254.
20. **Kancherla, V. S., and I. C. Hanson.** 2006. Mumps resurgence in the United States. J. Allergy Clin. Immunol. **118:**938–941.
21. **Kilham, L., and J. R. Overman.** 1953. Natural pathogenicity of mumps virus for suckling hamsters on intracerebral inoculation. J. Immunol. **70:**147–151.
22. **Kovamees, J., R. Rydbeck, C. Orvell, and E. Norrby.** 1990. Hemagglutinin-neuraminidase (HN) amino acid alterations in neutralization escape mutants of Kilham mumps virus. Virus Res. **17:**119–129.
23. **Kristensson, K., C. Orvell, G. Malm, and E. Norrby.** 1984. Mumps virus infection of the developing mouse brain—appearance of structural virus proteins demonstrated with monoclonal antibodies. J. Neuropathol. Exp. Neurol. **43:**131–140.
24. **Love, A., R. Rydbeck, K. Kristensson, C. Orvell, and E. Norrby.** 1985. Hemagglutinin-neuraminidase glycoprotein as a determinant of pathogenicity in mumps virus hamster encephalitis: analysis of mutants selected with monoclonal antibodies. J. Virol. **53:**67–74.
25. **Mazhul', L. A., and O. N. Ageeva.** 1983. Enzyme activity of the neuraminidase from various strains of the influenza A virus. Vopr. Virusol. **28:**43–46. (In Russian.)
26. **Merz, D. C., A. C. Server, M. N. Waxham, and J. S. Wolinsky.** 1983. Biosynthesis of mumps virus F glycoprotein: non-fusing strains efficiently cleave the F glycoprotein precursor. J. Gen. Virol. **64:**1457–1467.
27. **Merz, D. C., and J. S. Wolinsky.** 1981. Biochemical features of mumps virus neuraminidases and their relationship with pathogenicity. Virology **114:**218–227.
28. **Mori, C., T. Tooriyama, T. Imagawa, and K. Yamanishi.** 1997. Nucleotide sequence at position 1081 of the hemagglutinin-neuraminidase gene in the mumps virus Urabe vaccine strain. J. Infect. Dis. **175:**1548–1549.
29. **Nagai, Y., H. D. Klenk, and R. Rott.** 1976. Proteolytic cleavage of the viral glycoproteins and its significance for the virulence of Newcastle disease virus. Virology **72:**494–508.
30. **Orvell, C.** 1984. The reactions of monoclonal antibodies with structural proteins of mumps virus. J. Immunol. **132:**2622–2629.
31. **Paterson, R. G., and R. A. Lamb.** 1990. RNA editing by G-nucleotide insertion in mumps virus P-gene mRNA transcripts. J. Virol. **64:**4137–4145.
32. **Rafiefard, F., B. Johansson, T. Tecle, and C. Orvell.** 2005. Characterization of mumps virus strains with varying neurovirulence. Scand. J. Infect. Dis. **37:**330–337.
33. **Rubin, S. A., G. Amexis, M. Pletnikov, Z. Li, J. Vanderzanden, J. Mauldin, C. Sauder, T. Malik, K. Chumakov, and K. M. Carbone.** 2003. Changes in mumps virus gene sequence associated with variability in neurovirulent phenotype. J. Virol. **77:**11616–11624.
34. **Rubin, S. A., M. Pletnikov, and K. M. Carbone.** 1998. Comparison of the neurovirulence of a vaccine and a wild-type mumps virus strain in the developing rat brain. J. Virol. **72:**8037–8042.
35. **Rubin, S. A., M. Pletnikov, R. Taffs, P. J. Snoy, D. Kobasa, E. G. Brown, K. E. Wright, and K. M. Carbone.** 2000. Evaluation of a neonatal rat model for prediction of mumps virus neurovirulence in humans. J. Virol. **74:**5382–5384.
36. **Rubin, S. A., P. J. Snoy, K. E. Wright, E. G. Brown, P. Reeve, J. A. Beeler, and K. M. Carbone.** 1999. The mumps virus neurovirulence safety test in Rhesus monkeys: a comparison of mumps virus strains. J. Infect. Dis. **180:**521–525.

37. **Sauder, C. J., K. M. Vandenburgh, R. C. Iskow, T. Malik, K. M. Carbone, and S. A. Rubin.** 2006. Changes in mumps virus neurovirulence phenotype associated with quasispecies heterogeneity. Virology **350:**48–57.
38. **Sinclair, C., M. Mirakhur, J. Kirk, M. Farrell, and S. McQuaid.** 2005. Up-regulation of osteopontin and αβ-crystallin in the normal-appearing white matter of multiple sclerosis: an immunohistochemical study utilizing tissue microarrays. Neuropathol. Appl. Neurobiol. **31:**292–303.
39. **Smorodintsev, A. A., M. N. Nasibov, and N. V. Jakovleva.** 1970. Experience with live rubella virus vaccine combined with live vaccines against measles and mumps. Bull. W. H. O. **42:**283–289.
40. **Tanabayashi, K., K. Takeuchi, K. Okazaki, M. Hishiyama, and A. Yamada.** 1992. Expression of mumps virus glycoproteins in mammalian cells from cloned cDNAs: both F and HN proteins are required for cell fusion. Virology **187:**801–804.
41. **Tecle, T., B. Bottiger, C. Orvell, and B. Johansson.** 2001. Characterization of two decades of temporal co-circulation of four mumps virus genotypes in Denmark: identification of a new genotype. J. Gen. Virol. **82:**2675–2680.
42. **Tecle, T., A. Mickiene, B. Johansson, L. Lindquist, and C. Orvell.** 2002. Molecular characterisation of two mumps virus genotypes circulating during an epidemic in Lithuania from 1998 to 2000. Arch. Virol. **147:**243–253.
43. **Tesovic, G., J. Begovac, and A. Bace.** 1993. Aseptic meningitis after measles, mumps, and rubella vaccine. Lancet **341:**1541.
44. **Vesikari, T., F. E. Andre, E. Simoen, G. Florent, E. L. Ala-Laurila, A. Heikkinen, H. Kuusinen, and A. Terho.** 1983. Evaluation in young children of the Urabe Am 9 strain of live attenuated mumps vaccine in comparison with the Jeryl Lynn strain. Acta Paediatr. Scand. **72:**37–40.
45. **Waxham, M. N., and J. Aronowski.** 1988. Identification of amino acids involved in the sialidase activity of the mumps virus hemagglutinin-neuraminadase protein. Virology **167:**226–232.
46. Reference deleted.
47. **WHO.** 1994. WHO Expert Committee on Biological Standardization. WHO Tech. Rep. Ser. **840:**1–218.
48. **Wilson, R. L., S. M. Fuentes, P. Wang, E. C. Taddeo, A. Klatt, A. J. Henderson, and B. He.** 2006. Function of small hydrophobic proteins of paramyxovirus. J. Virol. **80:**1700–1709.
49. **Wolinsky, J. S.** 1996. Mumps virus, p. 1243–1265. *In* B. N. Fields, D. M. Knipe, and P. M. Howley (ed.), Fields virology. Lippincott-Raven, Philadelphia, PA.
50. **Wolinsky, J. S., T. Klassen, and J. R. Baringer.** 1976. Persistence of neuroadapted mumps virus in brains of newborn hamsters after intraperitoneal inoculation. J. Infect. Dis. **133:**260–267.
51. **Wolinsky, J. S., and W. G. Stroop.** 1978. Virulence and persistence of three prototype strains of mumps virus in newborn hamsters. Arch. Virol. **57:**355–359.